

## Engineering of composite metallic microfibers towards development of plasmonic devices for sensing applications

This content has been downloaded from IOPscience. Please scroll down to see the full text.

2016 IOP Conf. Ser.: Mater. Sci. Eng. 108 012027

(<http://iopscience.iop.org/1757-899X/108/1/012027>)

View [the table of contents for this issue](#), or go to the [journal homepage](#) for more

### Download details:

IP Address: 152.78.74.178

This content was downloaded on 04/10/2016 at 16:05

Please note that [terms and conditions apply](#).

You may also be interested in:

[Organ Printing: In vitro tissue/organ models](#)

D-W Cho, J-S Lee, J Jang, J W Jung, J H Park and F Pati

[Preparation of potato starch microfibers obtained by electro wet spinning](#)

W Cárdenas, E Y Gómez-Pachon, E Muñoz et al.

[Liquid Concentration Sensing Properties of Microfibers with a Nanoscale-Structured Film](#)

Zhou Guo-Rui, Lv Hai-Bing, Yuan Xiao-Dong et al.

[Carbon Microfibers Grown on Graphite Electrode During Fullerene Generation Using Composite Graphite Rods](#)

Masafumi Ata, Yasunori Kijima, Hiroshi Imoto et al.

[Preparation of Curled Microfibers by Electrospinning with Tip Collector](#)

Tang Cheng-Chun, Chen Jun-Chi, Long Yun-Ze et al.

[Fabrication and Characterization of a 2 × 2 Microfiber Knot Resonator Coupler](#)

A. A. Jasim, A. Z. Zulkifli, M. Z. Muhammad et al.

[Solution concentration and refractive index sensing based on polymer microfiber knot resonator](#)

Huaqing Yu, Liangbin Xiong, Zhihong Chen et al.

# Engineering of composite metallic microfibers towards development of plasmonic devices for sensing applications

A Petropoulou<sup>1,3</sup>, G Antonopoulos<sup>1</sup>, P Bastock<sup>2</sup>, C Craig<sup>2</sup>, G Kakarantzas<sup>1</sup>,  
D W Hewak<sup>2</sup>, M N Zervas<sup>2</sup>, C Riziotis<sup>1</sup>

<sup>1</sup> Theoretical and Physical Chemistry Institute, Photonics for Nanoapplications Laboratory, National Hellenic Research Foundation, Athens 116 35, Greece

<sup>2</sup> Optoelectronics Research Centre, University of Southampton, Southampton SO17 1BJ, United Kingdom

<sup>3</sup> Department of Informatics and Telecommunications, University of Peloponnese, Tripolis 22100, Greece

E-mail: apetropoulou@eie.gr, Riziotis@eie.gr, M.N.Zervas@soton.ac.uk

**Abstract.** The paper discusses the analysis of tapered hybrid composite microfibers based on a metal-core and dielectric-cladding composite material system. Its advantages over the pure metal tips conventionally used, are the inherent enhanced environmental robustness due to inert borosilicate cladding and the capability of multiple excitation of the tapered nanowire through the length of the fiber due to the enabled total internal reflection at the borosilicate/air interface. Simulations through finite element method (FEM) have demonstrated an improved field enhancement at the tapered region of such microfibers. Furthermore, experimental results on tapering in copper based microfibers together with light coupling and propagation studies will be demonstrated revealing the potential for the development of plasmonic devices for sensing applications.

## 1. Introduction

Surface plasmon polaritons (SPPs) are surface electromagnetic waves travelling along a metal/dielectric interface, whose field decays exponentially in both media. SPPs have attracted great interest and have found many applications in biosensing, surface-enhanced Raman spectroscopy (SERS) and also microscopy, since they offer high field enhancement and confinement beyond the diffraction limit [1].

The field enhancement at the apex of metallic tips have been extensively studied theoretically [2-4], however it has been clearly identified lately the need for further research towards the engineering of physically realizable and robust plasmonic structures with enhanced performance. In this study the performance of tapered hybrid copper-core/borosilicate-cladding microfiber is analyzed. Their advantages over the metal tips are the absence of impurities and the multiple excitation of the nanowire through the length of the fiber due to the repeated total internal reflection at the silicate/air interface [5]. High field enhancement is expected at the apex of such tapers.



## 2. Modelling

For metallic core nano-wires of radius  $R_1$  surrounded by a dielectric layer of radius  $R_2$ , the amplitudes of the electric and magnetic fields for TM<sub>01</sub> mode [6] are:

$$E(\rho) = \begin{cases} A_1 \left[ -i \left( \frac{\beta}{\alpha_1} \right) I_1(\alpha_1 \rho) \hat{e}_\rho + I_0(\alpha_1 \rho) \hat{e}_z \right], & \rho \leq R_1 \\ \left( \frac{\beta}{\alpha_2} \right) [-i A_2 I_1(\alpha_2 \rho) + B_2 K_1(\alpha_2 \rho)] \hat{e}_\rho + [A_2 I_0(\alpha_2 \rho) - i B_2 K_0(\alpha_2 \rho)] \hat{e}_z, & R_1 \leq \rho \leq R_2 \\ A_3 \left[ \left( \frac{\beta}{\alpha_3} \right) K_1(\alpha_3 \rho) \hat{e}_\rho - i K_0(\alpha_3 \rho) \hat{e}_z \right], & \rho \geq R_2 \end{cases} \quad (1)$$

$$H_\phi(\rho) = k \times \begin{cases} A_1 \left[ -i \left( \frac{\varepsilon_1}{\alpha_1} \right) I_1(\alpha_1 \rho) \right], & \rho \leq R_1 \\ \left( \frac{\varepsilon_2}{\alpha_2} \right) [-i A_2 I_1(\alpha_2 \rho) + B_2 K_1(\alpha_2 \rho)], & R_1 \leq \rho \leq R_2 \\ A_3 \left[ \left( \frac{\varepsilon_3}{\alpha_3} \right) K_1(\alpha_3 \rho) \right], & \rho \geq R_2 \end{cases} \quad (2)$$

where  $\beta$  is the propagation constant,  $\varepsilon_1$ ,  $\varepsilon_2$  and  $\varepsilon_3$  are the relative permittivities of metal core, dielectric cladding and air respectively,  $\alpha_j = (\beta^2 - \varepsilon_j k^2)^{1/2}$  for  $j=1,2,3$ , I and K are the modified Bessel functions of the first and second kinds and  $A_1$ ,  $A_2$  and  $A_3$  are the complex constants.

The dispersion equation can be derived by the continuity of the tangential components of the fields at the interfaces  $\rho = R_1$  and  $\rho = R_2$ :

$$\begin{aligned} & \varepsilon_1 \alpha_2 I_1(\alpha_1 R_1) [\alpha_2 \varepsilon_3 K_1(\alpha_3 R_2) M_{00} + \alpha_3 \varepsilon_2 K_0(\alpha_3 R_2) M_{10}] = \\ & -\varepsilon_2 \alpha_1 I_0(\alpha_1 R_1) [\alpha_2 \varepsilon_3 K_1(\alpha_3 R_2) M_{01} + \alpha_3 \varepsilon_2 K_0(\alpha_3 R_2) M_{11}] \end{aligned} \quad (3)$$

where  $M_{ab} = I_a(\alpha_2 R_2) K_b(\alpha_2 R_1) - (-1)^{a+b} I_b(\alpha_2 R_1) K_a(\alpha_2 R_2)$ .

Figures 1 and 2 show the real and imaginary part of the effective refractive index ( $n_{\text{eff}}$ ) as a function of the wavelength for different radii of the copper core. As the radius of the copper tip decreases, both the real and imaginary parts of  $n_{\text{eff}}$  increase. This means that, toward the apex of the metal tip, the effective wavelength of the plasmon wave decreases and the losses increase. For radii of the metal tip larger than 50nm the losses are relatively low. As the radius decreases the losses become significant and they are minimum for wavelength around 800nm.

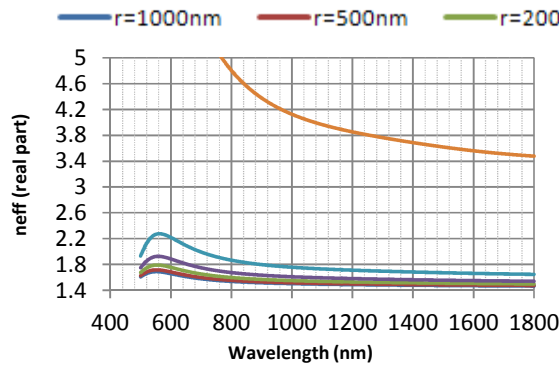


**Figure 1.** Real part of the effective refractive index ( $n_{\text{eff}}$ ) as a function of the wavelength for different radii of the copper core.

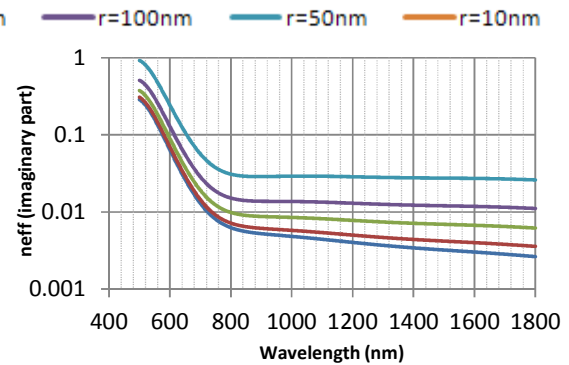


**Figure 2.** Imaginary part of the effective refractive index ( $n_{\text{eff}}$ ) as a function of the wavelength for different radii of the copper core.

### 2.1. FEM simulations of tapered composite microwire

The simulated structure is a copper cone with semi-angle,  $\alpha=3.43^\circ$ , input radius of  $r_{\text{input}}=150\text{nm}$  and output radius  $r_{\text{output}}=3\text{nm}$  to avoid singularities. The cone is surrounded by a borosilicate layer with a thickness that decreases so that the ratio of outer radius/core radius remains constant ( $\sim 12.5$ ). The launched mode is  $\text{TM}_{01}$  ( $P_{\text{input}}=1\text{W}$ ) and the transmission is along the  $z$  direction. Figure 3 shows the maximum normalized electric field at the apex of the tip as a function of the wavelength. We observe that periodic peaks appear in the field enhancement spectrum. These peaks appear when the tip length is more than  $1\text{ }\mu\text{m}$  due to SPPs that propagate along the tip. When the SPPs meet the end of the tip, they are reflected and form cavity modes [7].

The highest enhancement factor, defined as the maximum intensity  $I$  at the apex of the tip divided by the intensity  $I_o$  at the copper/borosilicate surface at the input of the fiber tip, is  $\sim 1.1 \times 10^4$  for  $\lambda=837\text{nm}$  (Fig. 4).

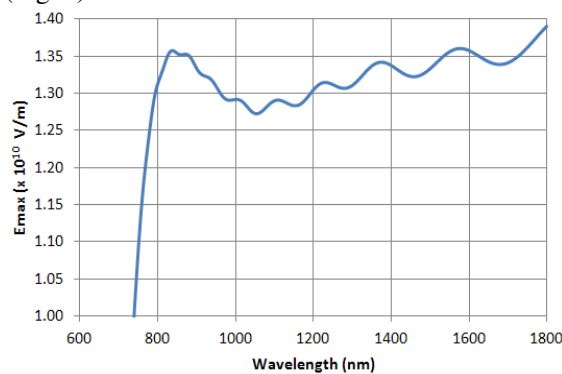


**Figure 3.** The maximum normalized electric field at the apex of the tip as a function of the wavelength.

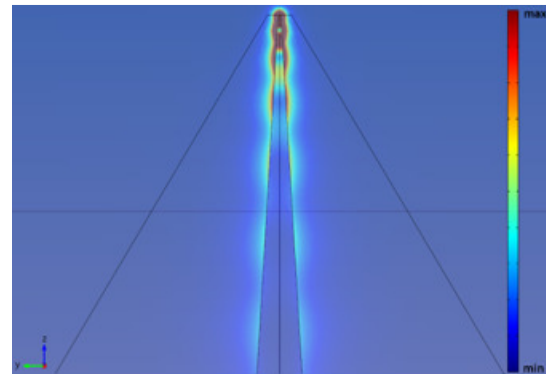


**Figure 4.** Normalized electric field for  $\lambda=837\text{nm}$ .

### 3. Experimental

The hybrid metal-core/dielectric-cladding microfibers that we used (Fig. 5), manufactured within the ORC [8], have copper core and borosilicate cladding with diameters of  $2\text{ }\mu\text{m}$  and  $25\text{ }\mu\text{m}$ , respectively. The nanowires are excited by coupling light of  $671\text{nm}$  into the silicate enclosure. As expected we observe two peaks in the 2D beam profile at the copper/silica interface for the fundamental mode (Fig.6). The two observed peaks correspond in good agreement to the illustrated modelled mode profile. In order to obtain the beam profile we used a  $60\times$  objective lens to image the near-field intensity distribution at the fiber output and a scanning slit optical beam profiler.

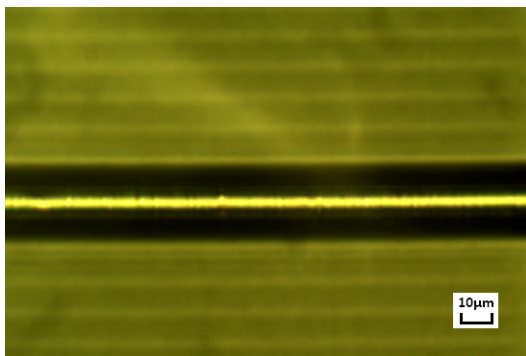


**Figure 5.** Microscope image of copper core micro-wire with borosilicate cladding.

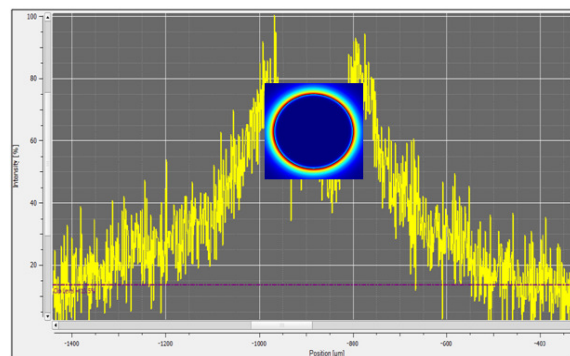


**Figure 6.** Beam profile of a hybrid microfiber and the corresponding modelled  $\text{TM}_{01}$  mode profile.

### 3.1. Tapering process

The microfiber was tapered with the method of heating and stretching [9]. Two linear stages stretch the microfiber while a third one moves the flame along the fiber axis (Fig. 7). Due to the low melting point of copper the fast and cold method was used in order to avoid the breakdown of the microfiber. The final waist radius of the copper core and the final waist length was 200nm and 13mm, respectively (Fig. 8).

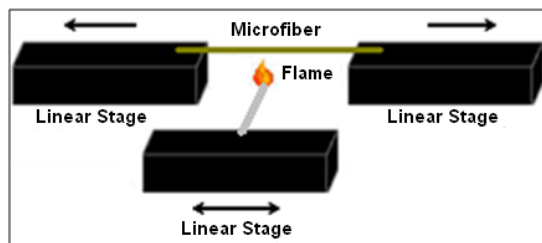


**Figure 7.** Schematic representation of the fiber tapering rig.

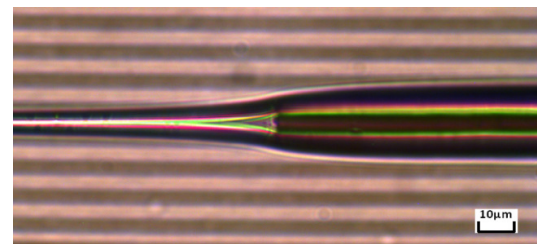


**Figure 8.** Microscope image of a tapered microfiber after the end of the tapering process.

## 4. Conclusions

The demonstrated results suggest that the hybrid copper-core/dielectric cladding microfibers are a very promising platform that can provide high field enhancement and confinement. The field enhancement expected at the apex of these tips is  $E_f \sim 1.1 \times 10^4$  at  $\lambda = 837\text{nm}$  making their use for sensing applications feasible. Their advantage over bare metal tips used is their low loss due to multiple reflections at the borosilicate/air interface that can provide higher intensities at their apex. We were able to taper them down to a core radius of 200nm using the heating and stretching method. Further research is ongoing for the optimization of the tapering conditions in a variety of metal-silicate composite systems, in order to achieve uniform and extremely thin tapered microfibers with optimised field enhancement.

## Acknowledgements

This work was funded by the General Secretariat for Research and Technology, Greece (Project Polynano-Kripis 447963).

## References

- [1] Stockmann M I 2011 *Opt. Express* **19** 22029
- [2] Stockmann M I 2004 *Phys. Rev. Lett.* **93** 137404
- [3] Uebel P, Bauerschmidt S T, Schmidt M A and Russell P St J 2013 *Appl. Phys. Lett.* **103** 021101
- [4] Zaccaria R P, Alabastri A, De Angelis F, Das G, Liberale C, Toma A, Giugni A, Razzari L, Malerba M, Sun H B and Di Fabrizio E 2012 *Phys. Rev. B* **86** 035410
- [5] Gholipour B, Nalla V, Bastock P, Khan K, Craig C, Hewak D W, Zheludev N I and Soci C 2014 *CLEO '14*
- [6] Handapangoda D, Premaratne M, Rukhlenko I D and Jagadish C 2011 *Opt. Express* **19** 16058
- [7] Zhang W, Cui X and Martin O J F 2009 *J. Raman Spectrosc.* **40** 1338
- [8] Bastock P. 2015 "Manufacturing Novel Fibre", *Doctor of Philosophy*. Optoelectronics Research Centre, University of Southampton.
- [9] Birks T A, Wadsworth W J and Russell P St J 2000 *Opt. Lett.* **25** 1415